Luo J. (2024) BIOMEDICAL DATA ANALYSIS OF JUMP MECHANICS IN TRACK AND FIELD ATHLETES AND ITS EFFECT ON INJURY. Revista Internacional de Medicina y Ciencias de la Actividad Física y el Deporte vol. 24 (98) pp. 77-89.
DOI: https://doi.org/10.15366/rimcafd2024.98.006

ORIGINAL

BIOMEDICAL DATA ANALYSIS OF JUMP MECHANICS IN TRACK AND FIELD ATHLETES AND ITS EFFECT ON INJURY

Jie Luo

Physical Education College of Chengdu University, Chengdu, Sichuan, 610106, China
E-mail: 18048051911@163.com

Recibido 05 de enero de 2024 **Received** January 05, 2024
Aceptado 09 de septiembre de 2024 **Accepted** September 09, 2024

ABSTRACT

The jumping action plays a very important role in many sports in athletics. Jumping action depends on explosive force, which is the quality of strength in a short period of time, and is the important basic quality of many sports. Mechanical research on jumping movement can explore ways to improve sports performance from the perspective of mechanics, and can also explore effective measures to prevent sports injuries. Biomedical data analysis can analyze a large amount of data in depth and reveal the rules behind the huge data. In this paper, biomedical analysis technology is used to analyze the mechanical data of track and field jumping movements, to explore the mechanical characteristics of high jumping movements and the intrinsic connection between movements and injuries, and good results are achieved.

KEYWORDS: Biomedical Data Analysis; Jump Mechanics; Injury

1. INTRODUCTION

Among the special training of track and field, the status of strength quality is particularly important (Maity & Das, 2022). Explosive force belongs to the speed power, is a short time power quality, is the important basic quality of many sports. It is related to the speed of movement, jumping and the ability to change course, and is an important influence factor in determining the winners and losers of the game and the performance of the sport. Athletics jumping sports belong to the physical dominance of the speed and power type item group, including distance (long jump, triple jump) and height items (high jump, pole vault), so jumping sports athletes should have in addition to good flexibility, bouncing power, but also have a certain speed quality and explosive force (Wang, Kurillo, Ofli, & Bajcsy, 2015). Jumping sports program with its unique requirements and characteristics, in the training and competition process is very easy to occur sports injuries (Rehm & Moradali, 2018; Shi, Xu, Pan, Yan, & Zhang, 2018). The jumping program generally consists of four parts, namely, running, jumping, vacating and landing, the body vacates and the ground to form a reaction force, at this time the knee joints and ankle joints and the waist and abdomen become the largest point of force (Z. Zhang et al., 2022). The most injured parts of jumping athletes are knee joints, followed by ankles, feet and waist. In jumping sports, the knee joint needs to yield and stirrup extension to get fast jumping speed, the force point is concentrated in the knee joint, which produces a large load on the knee joint, and over time causes the cartilage of the knee joint surface to wear out, resulting in knee osteoarthritis and meniscus injury. Patella not only to protect the stability of the joint, but also to extend the knee force, patella repeated wear and tear prone to chondromalacia patella. Jumping projects on the waist strength and flexibility requirements are also very high, the need for athletes to jump in the air for twisting, turning, jerking and other actions, so that the lumbar region to withstand a greater load resulting in lumbar injury (Pachella, 2021). With the development of information technology in the medical field, more and more human biometric data are acquired for storage and utilization. The content of the data includes the data of previous drug use, disease history data, blood pressure, weight, doctor's consultation data, medical image data, blood data, various hormone data, and part of the genetic data. It is believed that with the advancement of technology in the medical field, more and more human biometric data can be collected. These biomedical data themselves contain a large amount of information, which on the one hand can be utilized to help the relevant personnel to determine the health status of the human body and to screen for relevant diseases by utilizing the knowledge of medical experience. On the other hand, it can help researchers to study specific diseases in the human body characteristic reaction performance, and further study the principle of disease (Kong et al., 2020; Lloyd & Oliver, 2012). In recent years, with the rise of artificial neural network model, especially in many fields such as biomedical polymer sequence analysis, medical image analysis and auxiliary diagnosis, it has achieved very good experimental results (McClelland, 1979; Sahoo & Biswal, 2021). Compared with expert systems, deep neural networks have the advantages of self-learning ability, associative memory and fault tolerance, especially parallel processing, high efficiency and high accuracy. Meanwhile, the advantages of neural network system are more prominent than the traditional expert system in classification diagnosis and intelligent control and optimization solution based on classification. Although the classification method of neural network has achieved good classification effect, it depends on the model parameters to a large extent, and it is difficult to avoid the problem of model "overfitting" (X. Zhang, Shan, Wang, Wan, & Li, 2019). Deep neural networks were used to analyze the biomedical data on mechanics of jumping movements in track and field, to examine the mechanical characteristics of jumping movements from a new perspective, and to improve the understanding of jumping movements from different directions. At the same time, injury research is integrated into it to explore the relationship between jumping movements and injuries. In this paper, we take high jump as the research object, and use the deep neural network model to analyze the biomedical data of high jump mechanics, in order to understand the connection between high jump and injury (Datta, Barua, & Das, 2019; Maia, 2023; Sternberg, 1969).

2. Methodology

2.1 Human Body Modeling

By constructing the three-dimensional skeleton model of the athlete, its three-dimensional characteristic points can be obtained. Therefore, the high jumper is regarded as a collection of rigid bodies connected by joints, and the connection relationship between joints is represented by line segments. The motion of high jump is simplified into the motion of the athlete's skeleton, and the three-dimensional human skeleton model is obtained, which is described by the following Figure 1, and the coordinates of the joints in the model, are called the three-dimensional characteristic points.

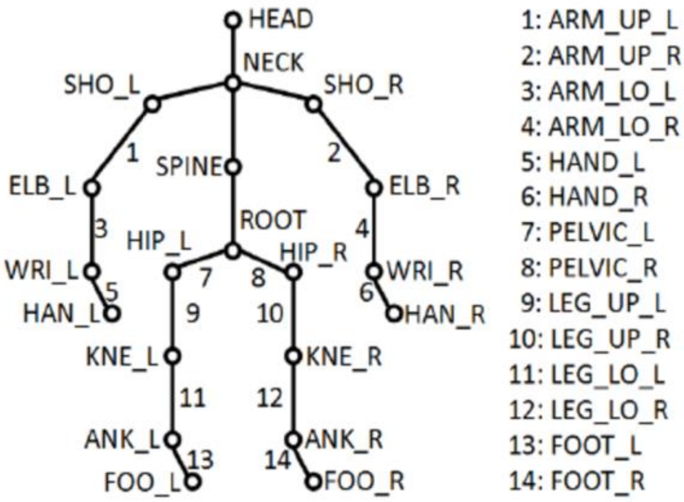

Figure 1: Three-dimensional skeleton (Lloyd et al., 2016).

In this paper, only five of the important body joints of the athlete are used for the calculation, which are: the left ear, the left shoulder, the left hip, the left toe, and the center of mass of the body five objects. They are abstracted into five nodes and the coordinate position data are embedded into our model for calculation. Our goal is to predict the position of joint points during a high jump. We assume the existence of N joints, denoted as $p_1, p_2, \cdots, p_N$ body joints $p_i (i \in [1, N])$ at time step t the position of the joints labeled as $S_i^t =$

(x_i^t, y_i^t, z_i^t). $S_i^t(i = 1,2,\cdots,N)$ denotes the position of the joints at time step $t = 1,\cdots,T_{obs}$, our goal is to predict the future position of the S_i^t at time step $t = T_{obs} + 1$, $\cdots$, $T_{obs} + T_{pred}$. In this paper we choose $T_{obs} = 6$, $T_{pred} = 6$,i.e., set up a sliding window with a sliding step of 1 each time, and use the coordinates of the joint positions in the first 6 moments of each window to predict the coordinates of the joint positions in the next 6 moments.

2.2 Analysis of High Jump Movement Patterns

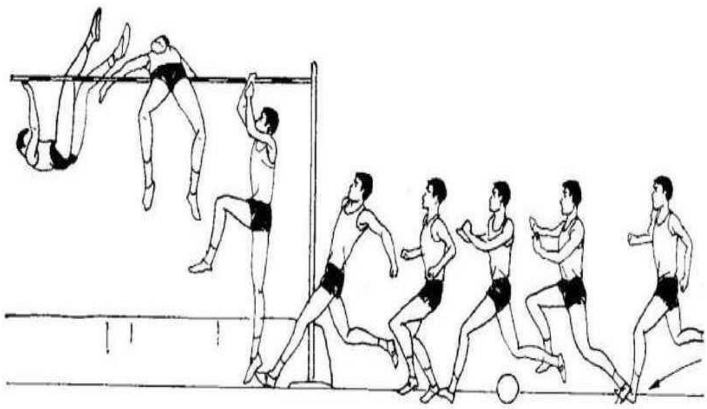

Figure 2: The backward high jump.

The process of jumping for a high jump can be divided into several states of motion at discrete points in time, as shown in the Figure 2. The states of motion include the position of the joints of the athletes at this moment in time, their speeds, and so on. Considering the process of high jump as a physical system, the trajectory of the future moment is determined by the trajectory and state of the historical moment, so the trajectory of high jump is a complex temporal causal and nonlinear relationship. We utilize the information of the athlete's state in the historical time point to infer the trajectory of the athlete in several future moments. Therefore, the high jump trajectory prediction problem can be regarded as a complex sequence prediction problem, in which the positions of the athlete's joints at the given previous moments are predicted to infer the positions of the athlete's joints at the next moments.

$$S^{t+T} = f(S^{t-1}, S^{t-2}, \cdots, S^{t-T_{obs}}, \theta_k), T = 0,1,2,\cdots,T_{pred}, k = 0,1,2,\cdots,K \tag{1}$$

$$S_i^t = (x_i^t, y_i^t, z_i^t), i = 1,2,3,4,5 \tag{2}$$

$$S^t = [S_1^t, S_2^t, S_3^t, S_4^t, S_5^t] \tag{3}$$

$$g(S_1^t, S_2^t, S_3^t, S_4^t, S_5^t, \theta_k) \leq 0, k = 0,1,2,\cdots,K \tag{4}$$

Where S^t denotes the position of the athlete's body joints at moment t T_{pred} forward predicted moments, T_{obs} the number of historical moments observed, i.e., for a certain moment i, the high jump movement state and trajectory of the previous moment is used to predict the movement trajectory of the future T_{pred} moment.θ_k denotes the parameters related to the movement trajectory, and K denotes the number of parameters. f denotes the pattern of the high jump movement trajectory. S_i^t denotes the position of the athlete's joint points at the moment of t, where $i = 1,2,3,4,5$ denotes the left ear, the left shoulder, the left hip, the left toe, and the center of mass of the body, respectively.g denotes the limitation of the swing range of the body joints to each other, and the degree to which the swing amplitude of the joints is influenced by the other joints. In the following, we consider a spatio-temporal graphical neural network model to portray this movement pattern.

2.3 STGAT Network Architecture

The STGAT network model is used. Its structure is built around the seq2seq model and consists of three components: an encoder, an intermediate state, and a decoder. The Encoder module is made up of three parts: two types of LSTMs and a GAT. LSTMs are included in the original STGAT structure, and in this paper, we express the original STGAT as STGAT-LSTM, whereas the spatio-temporal graph neural network (Encoder module) in the original STGAT structure is expressed as STGAT. The intermediate state contains all nodes' temporal and geographical information. Based on the intermediate states, the decoder module generates future trajectories. We embed the position of the body joints at the time step t, $S_i^t = (x_i^t, y_i^t, z_i^t)$, cure data into the network as input to the Encoder module. The architecture of the STGAT network is shown in Figure 3.

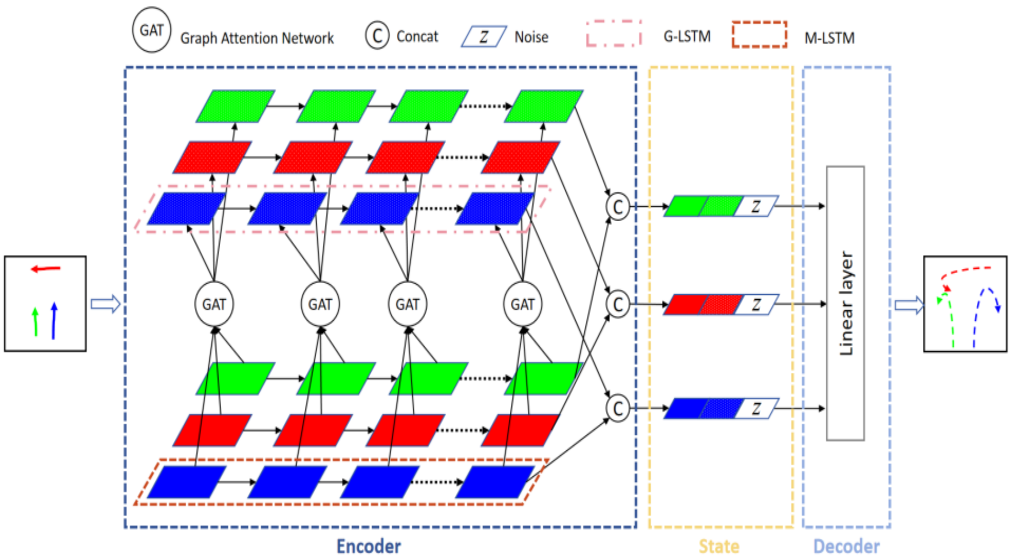

Figure 3: STGAT network structure (Santamaria & Webster, 2010).

2.4 Motion Encoder: M-LSTM

Each node has its own motion pattern, which includes various displacements, velocities, accelerations, and so on. It has been demonstrated that LSTM can more successfully capture the historical motion trajectory of a single node (Snodgrass, Luce, & Galanter, 1967). As a result, we employ an LSTM for each node to capture its motion state, and this LSTM is denoted by M-LSTM. The node position S_i^t is embedded into a fixed-length vector e_i^t and this vector is used as an input to the LSTM unit:

$$e_i^t = \phi(x_i^t, y_i^t, z_i^t; W_{ee}) \tag{5}$$

$$m_i^t = MLSTM(m_i^{t-1}; e_i^t; W_m) \tag{6}$$

where $\phi(\cdot)$ denotes an embedding function and W_{ee} is the embedding weight. At time step t, the M-LSTM's hidden state is m_i^t. These criteria apply to all joints. The M-LSTM weights are W_m, and these parameters are shared by all nodes.

2.5 Graph Attention Networks

Using only one LSTM does not capture the interaction between body joint points. In order to show the information during the jumping process, we consider the joint points of the high jumper as nodes on the graph and utilize the graph neural network approach (Quazi, Saha, & Singh, 2022). As GAT collects information from surrounding nodes by giving varying degrees of priority to each node. As a result, GAT is used as a spatial connection mechanism between joint sites. Edges on the graph are used to denote the presence of joints and the interactions between joints. Following this approach, the high jumper's joint points are treated as nodes on the graph in each time step. GAT acts on graph structure data and computes the features of each graph node by paying attention to its neighbors using a self-attentive technique. The GAT is built by superimposing graph attention layers. Figure 4 depicts the introduction of the graph attention layer.

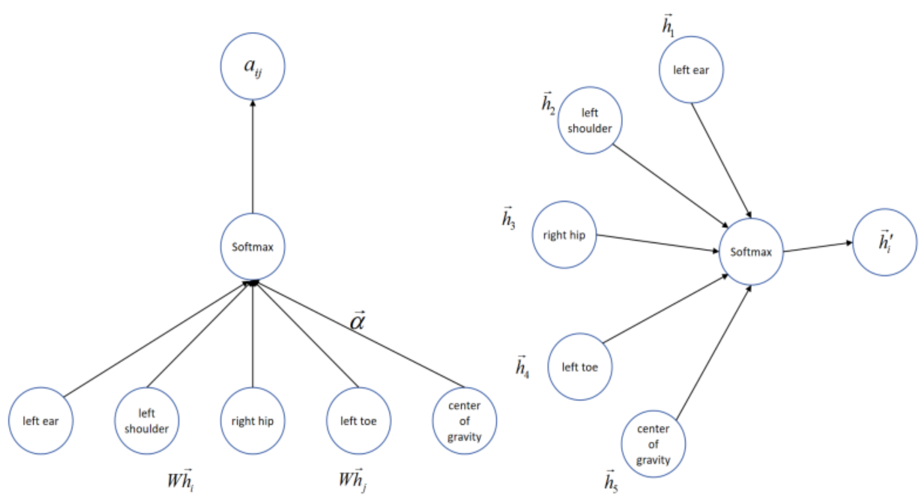

Figure 4: Schematic diagram of the structure of the attention layer.

The input to the graph attention layer is $h = \{\vec{h}_1, \vec{h}_2, \cdots, \vec{h}_N\}$, where $(h_i) \in R^F, N$ is the number of nodes and F is the per-node feature dimension. The output is $h' = \{\vec{h}'_1, \vec{h}'_2, cdots, \vec{h}'_N\}$, where ${h^{\vec{\prime}}_i}^{F'}$ is the number of nodes and F is the number of feature dimensions per node. ${h^{\vec{\prime}}_i}^{F'{}'}$ and F can be unequal. The coordinates of the joint points of the high jumper $m_i^t(t = 1, \cdots, T_{obs})$ are fed into the graph attention layer. The coefficients of the node (i, j)pairs in the attention mechanism will be calculated like this:

$$\alpha_{ij}^t \frac{exp\left(LeskyReLU\left(a^T\left[Wm_i^t \| Wm_j^t\right]\right)\right)}{\sum_{k\in N_i} exp\left(LeskyReLU\left(a^T\left[Wm_i^t \| Wm_j^t\right]\right)\right)} \tag{7}$$

Here ‖ is the connectivity operation, a^T denotes the transpose, α_{ij} is the attention coefficient of nodes j to i at time step t, atijatij is the attention coefficient of nodes j to i at time step t. Situations are the neighbors of node i on the wavenumber. $W \in R^{F' \times F}$ is the matrix of linear transformations shared by the weights for each node (F is the dimension of m_i^t and F' is the dimension of the outputs) and $a \in R^{2F'}$ is the vector of weights for a single-layer feed-forward neural network, normalized by the SoftMax function with LeakyReLU. After obtaining the normalized attention coefficients, the formula for the output of node i in the graph attention layer at time step t:

$$\widehat{m}_i^t = \sigma\left(\sum_{j\in N_i} \alpha_{ij}^t W m_j^t\right) \tag{8}$$

where σ is a nonlinear function. The above equation shows how a single graph attention layer works. In our scheme, four graph attention layers are used. $\widehat{m}_i^t$ (the output of the two graph attention layers) is the aggregated hidden state of node i at time step t, which contains spatial influences from other nodes.

2.6 Integration of Spatial and Temporal Information

Modeling spatio-temporal interaction processes in high jump sports scenarios, many LSTM-based methods. Only the information hidden at the same time step is considered. We use two LSTMs to model the interaction of explicit information, and we call this LSTM G-LSTM:

$$g_i^t = G - LSTM\left(g_i^{t-1}, \widehat{m}_i^t; W_g\right) \tag{9}$$

Where $\hat{m}_i^t$ is from Equation (8). W_g is the weight of the G-LSTM, which is shared among all sequences. Two LSTMs (M-LSTM and G-LSTM) represent the motion pattern of each joint point as well as the temporal correlation of the interaction in the encoder component. We integrate these two components to achieve spatial and temporal information fusion. At time step T_{obs}, for each athlete joint, two hidden variables $\left(m_i^{T_{obs}}, g_i^{T_{obs}}\right)$ are obtained by M-LSTM, G-LSTM. These two variables are then put into two different multilayer perceptual machines $\delta_1(\cdot)$ with $\delta_2(\cdot)$. Next, their outputs are connected:

$$\bar{m}_i = \delta_1\left(m_i^{T_{obs}}\right) \tag{10}$$

$$\bar{g}_i = \delta_2\left(g_i^{T_{obs}}\right) \tag{11}$$

$$h = \bar{m}_i \| \bar{g}_i \tag{12}$$

2.7 Prediction of High Jump Trajectories

We must learn the motion patterns of the high jump joint points from a genuine high jump trajectory dataset. We require models that can generate several reasonable and realistic trajectories due to the uncertainty in the mobility of the joint points. The majority of past work quantifies uncertainty by first learning the parameters of a Gaussian process and then deriving future positions taken from this distribution.

The model minimizes the negative log-likelihood loss of the true locations of the joints under the Gaussian distribution during the training phase. However, because the sampling procedure is not trivial, this approach presents issues in backpropagation. Our model's intermediate state vector is made up of three parts: the hidden variable M-LSTM, the hidden variable G-LSTM, and the added noise. The intermediate state vector is computed as:

$$d_i^{T_{obs}} = h_i \| z \tag{13}$$

where z denotes noise and h_i comes from equation (12). The intermediate state vector $d^{T_{obs}}$ is used as the initial hidden state of decoder $\delta_3(\cdot)$. The predicted relative position is given by equation: \

$$d_i^{T_{obs}+1} = \delta_3\left(d_i^{T_{obs}+1}\right) \ (14) \left(\Delta x_i^{T_{obs}+1}, \Delta y_i^{T_{obs}+1}, \Delta z_i^{T_{obs}+1}\right) = d_i^{T_{obs}+1} \quad (15)$$

where $\delta_3(\cdot)$ is a linear layer that passes the intermediate state variables through the $\delta_3(\cdot)$ linear layer to obtain the position coordinates of the predicted time step $T_{obs}+1$.

The losses due to different noises are as follows: for each node, the model generates multiple predicted trajectories by randomly sampling z from $N(0,1)$ (standard normal distribution). Then, we choose the smallest model loss:

$$L_{variety}=\min_{K}\frac{\sum_{t=1}^{N}\sum_{t=1}^{T_{pred}}\|\hat{Y}_l^t-Y_i^t\|}{NT_{pred}} \tag{16}$$

Where $Y_i$is the true trajectory of the athlete's joint i, $\hat{Y}_l^k$ is the trajectory computed by the model, and K is a hyperparameter. By considering only the best trajectories, the network is enabled to satisfy the output space that conforms to the past trajectories.

3. Model Validation Experiments

3.1 Data Description

The data in this paper are the seven high jump competition data of a professional high jumper. The data were collected from the video shot by the camera at the competition site, and analyzed by the high jump video software to get the 3D coordinates of the 21 joints and important parts of the athlete as well as the center of mass from the start of the run-up step to the airborne stage at intervals of 0.02 seconds. There are about 70 time points of each important body parts of the three-dimensional coordinate data. The data are time series data, each time point data interval is 0.02 seconds.

3.2 Analysis of Evaluation Indicators

We use the data from the first 6 races to train the model. The data from the last competition is used for testing. The baseline models chosen in this paper are: LSTM, GRU, STGAT-LSTM, STGAT-GRU. The evaluation metric we chose is the Average Displacement Error (ADE) of the sliding window prediction multiple times: the mean square error of all the estimated positions in the predicted trajectory and the true trajectory. the mean square error of all estimated positions in the trajectory.

$$ADE=\frac{\sum_{t=1}^{N}\sum_{t=1}^{T_{pred}}\|\hat{Y}_l^t-Y_i^t\|}{F*N*T_{pred}} \tag{17}$$

Where Y_i is the true trajectory of the athlete's joint i, $\hat{Y}_l^k$ is the trajectory computed by the model, and F is the coordinate dimension of the node 3. The model predictions are shown in Table 1 .

Table 1: Model prediction results.

Models	ADE(m)
LSTM	0.0588
STGAT LSTM	0.0379
GRU	0.0640
STGAT GRU	0.0298

From the experimental results, the prediction effect of the prediction model combining the graph attention layer is improved. In terms of the average position error in each direction, STGAT-LSTM reduces 0.0209 meters compared with the pure LSTM model, and STGAT-GRU reduces 0.0342 meters compared with the pure GRU. The high jump movement process is a complex system with mixed temporal and spatial information and interactions between joints, and the experimental results show that STGAT has certain advantages in processing and fusing spatial and temporal information.

4. Jumping Maneuvers and Injury Risk Studies

4.1 Methods of Analyzing Mechanical Data

Three-dimensional movement analysis technology can help researchers collect data during real-time movement and perform relevant biomechanical analyses (Trujillo et al., 2010), so scholars have widely utilized this movement technology analysis tool to explore the underlying mechanical factors that may lead to ACL injuries. Studies have shown that ACL injuries are commonly seen in movements such as the sharp stop and jump, lateral cut and change of direction, and jump-landing. Therefore, scholars mainly simulate these ACL injury-prone movements in the laboratory and use a 3D motion technology acquisition and analysis system to collect and analyze the biomechanical characteristics of the lower extremity during the execution of the movement to speculate the risk factors that may lead to ACL injuries or to identify the high-risk groups that are prone to ACL injuries.

Due to the variability of sports, the movements of athletes with ACL injuries also show a certain degree of variability. According to the existing literature, the jumping maneuver, the side-cutting change of direction maneuver, and the jump-landing maneuver are the main injury risk assessment maneuvers. The landing cushion phase is a high-risk phase for the occurrence of ACL injuries. Therefore, even though there are various maneuvers used to assess ACL injury risk, scholars have mainly studied the landing phase of various maneuvers.

4.2 Risk Prediction Studies for Jumping Movements and Injuries

Prospectively predicting people at high risk of ACL injury is also a hot research topic among scholars. Scholars mainly collect the biomechanical characteristics of the lower limbs when the subjects complete the landing movement and analyze them in order to predict those who may be at a higher risk of injury and intervene in time to reduce the risk of injury. However, from the current research, the results of scholars are not consistent, which makes some scholars believe that the laboratory test movement is not a good predictor of ACL injury risk. It is conducted the DJ movement test on 256 female athletes and followed up their injuries for two years, and concluded that the knee abduction moment can be a better predictor of ACL injury risk in female athletes, with sensitivity and specificity reaching 4.0% and 4.0%, respectively. They concluded that knee abduction moment was a good predictor of ACL injury risk in female athletes, with a sensitivity and specificity of 78% and 73%, respectively.

However, it did not observe an association between knee abduction moment and ACL injury risk in 1855 female athletes tested and followed up in the DJ maneuver, and it is found that knee inversion during the DJ maneuver was associated with an increased risk of ACL injury in young female athletes, but with poor sensitivity and specificity. This study also did not observe an association between knee abduction angle, knee abduction moment, knee flexion angle, and vGRF with ACL injury risk.Leppanen et al, however, concluded that knee flexion angle and peak vGRF were associated with the prediction of their ACL injury risk during DJ maneuvers, but also demonstrated poor sensitivity and specificity. This suggests a limitation in the applicability of the laboratory landing task in representing the motor strategy of jump landing movements in a specialized sport (Sport specific task). It also suggests that we need to use movements that are closer to those used in competition to predict people at high risk of ACL injury.

5. Conclusion

This paper adopts the biomedical data analysis method to construct a model using deep learning technology to predict and analyze the high jump movement from the mechanical point of view, to explore the mechanical characteristics of jumping action, and the relationship between jumping action and injury. It provides technical references for reducing the injuries received by track and field athletes due to jumping movements in training and competitions. It also provides a basis for coaches to scientifically formulate training programs and guide training.

REFERENCES

Datta, S., Barua, R., & Das, J. (2019). Application of artificial intelligence in modern healthcare system. *Alginates-recent uses of this natural polymer*.

Kong, X., Xing, W., Wei, X., Bao, P., Zhang, J., & Lu, W. (2020). STGAT: Spatial-temporal graph attention networks for traffic flow forecasting. *IEEE Access, 8*, 134363-134372.

Lloyd, R. S., Cronin, J. B., Faigenbaum, A. D., Haff, G. G., Howard, R., Kraemer, W. J., . . . Oliver, J. L. (2016). National Strength and Conditioning Association position statement on long-term athletic development. *The Journal of Strength & Conditioning Research, 30*(6), 1491-1509.

Lloyd, R. S., & Oliver, J. L. (2012). The youth physical development model: A new approach to long-term athletic development. *Strength & Conditioning Journal, 34*(3), 61-72.

Maia, D. (2023). Assessing the impact of commercial fishing on the abundance and diversity of fish species in a marine protected area: A empirical research in the Mediterranean Sea. *FishTaxa-Journal of Fish Taxonomy, 27*.

Maity, C., & Das, N. (2022). Alginate-based smart materials and their application: Recent advances and perspectives. *Topics in Current Chemistry, 380*(1), 3.

McClelland, J. L. (1979). On the time relations of mental processes: an examination of systems of processes in cascade. *Psychological review, 86*(4), 287.

Pachella, R. G. (2021). The Interpretation of reaction time in information-processing research 1. In *Human information processing* (pp. 41-82): Routledge.

Quazi, S., Saha, R. P., & Singh, M. K. (2022). Applications of artificial intelligence in healthcare. *Journal of Experimental Biology and Agricultural Sciences, 10*(1), 211-226.

Rehm, B. H., & Moradali, M. F. (2018). *Alginates and their biomedical applications* (Vol. 11): Springer.

Sahoo, D. R., & Biswal, T. (2021). Alginate and its application to tissue engineering. *SN Applied Sciences, 3*(1), 30.

Santamaria, L. J., & Webster, K. E. (2010). The effect of fatigue on lower-limb biomechanics during single-limb landings: a systematic review. *Journal of orthopaedic & sports physical therapy, 40*(8), 464-473.

Shi, Z., Xu, M., Pan, Q., Yan, B., & Zhang, H. (2018). *LSTM-based flight trajectory prediction.* Paper presented at the 2018 International joint conference on neural networks (IJCNN).

Snodgrass, J. G., Luce, R. D., & Galanter, E. (1967). Some experiments on simple and choice reaction time. *Journal of experimental psychology, 75*(1), 1.

Sternberg, S. (1969). Memory-scanning: Mental processes revealed by reaction-time experiments. *American scientist, 57*(4), 421-457.

Trujillo, A., Rojas, I., Pomares, H., Prieto, A., Prieto, B., Aránega, A., . . . Prados, J. C. (2010). *Analysis of the inducing factors involved in stem cell differentiation using feature selection techniques, support vector machines and decision trees.* Paper presented at the International

Conference on Industrial, Engineering and Other Applications of Applied Intelligent Systems.

Wang, Q., Kurillo, G., Ofli, F., & Bajcsy, R. (2015). Remote health coaching system and human motion data analysis for physical therapy with microsoft kinect. *arXiv preprint arXiv:1512.06492*.

Zhang, X., Shan, G., Wang, Y., Wan, B., & Li, H. (2019). Wearables, biomechanical feedback, and human motor-skills' learning & optimization. *Applied Sciences, 9*(2), 226.

Zhang, Z., Chen, L., Zhong, F., Wang, D., Jiang, J., Zhang, S., . . . Li, X. (2022). Graph neural network approaches for drug-target interactions. *Current Opinion in Structural Biology, 73*, 102327.